Supplemental Data

Symmetry-Breaking Polarization

Driven by a Cdc42p GEF-PAK Complex

Lukasz Kozubowski, Koji Saito, Jayme M. Johnson, Audrey S. Howell, Trevin R. Zyla, and

Daniel J. Lew

Supplemental Experimental Procedures

Yeast strains and plasmids

The *bem1::URA3* [1], *rsr1::HIS3* [2] and *bud8::TRP1* (previously *bud8-Δ1*) [3] disruptions were as previously described. *skm1::TRP1* and *ste20::URA3* were generated by the one-step PCR-based method [4] using pRS314 and pRS306 [5] as templates. *cla4::nat*^{R}, *ste20::hyg*^{R}, and *boi1::hyg*^{R} disruptions were generated similarly, using either pAG25 (*nat*^{R}) or pAG32 (*hyg*^{R}) as templates [6]. *boi1::kan*^{R}, *rsr1::kan*^{R} and *skm1::kan*^{R} gene disruptions were generated similarly, by PCR using genomic DNA from the ResGen deletion collection as template.

To express wild-type and mutant *BOI1* in yeast, we first cloned a 4.5 kb *Hind*III-*Bam*HI fragment containing the *BOI1* ORF together with 1.5 kb upstream and 0.4 kb downstream sequence from pPB1142 [7] into the corresponding sites of YCplac111 [8], yielding pDLB2648. Using overlap PCR, we replaced the proline-rich domain (from P394 to P413) with the sequence gcggccgct encoding three alanine residues and introducing a *Not*I site. Due to a primer error, there was also a 3 bp deletion removing residue N423. The resulting plasmid, pDLB2647, expresses *BOI1*$^{\Delta PxxP}$.

To express wild-type and mutant *STE20* in yeast, we first cloned a 4.3 kb *Spe*I-*Kpn*I fragment containing the *STE20* ORF together with 1.2 kb upstream and 0.26 kb downstream sequence from pPP2370 (kindly provided by Peter Pryciak) into *Xba*I- and *Kpn*I-digested YCplac111 [8], yielding pDLB2922. A *Sph*I-*Sgr*AI fragment containing promoter and N-terminal *STE20* sequences was replaced with the corresponding fragment from pPP1214 [9], in which Pro475 is changed to Gly and Pro477 is changed to Ala. The resulting plasmid, pDLB2923, expresses *STE20*$^{PP\text{-}GA}$. To generate plasmid DLB2921 containing *STE20*$^{PP\text{-}GA}$, a *Sph*I-*Sgr*AI fragment of pPP1214 was cloned into *Sph*I-*Sgr*AI-digested pPP2370. Plasmids expressing GFP-Ste20p (pRL116 [10]) and GFP-Ste20p$^{PP\text{-}GA}$ (pPP1211 [9]) were kindly provided by P. Pryciak.

To create a strain expressing *STE20*$^{PP\text{-}GA}$ at its genomic locus, a *ste20::hyg*^{R} strain was transformed with a 3.2 kb *Sph*I-*Kpn*I fragment of *STE20*$^{PP\text{-}GA}$ (extending from 0.15 kb upstream to 0.26 kb downstream of the ORF, derived after subcloning from pPP1214 [9]). Recombination between this fragment and the genomic locus to generate a precise replacement was screened for by loss of Hygromycin resistance, and confirmed by PCR.

To generate temperature-sensitive *cla4-td* strains, the plasmid p*cla4-td* [11] was digested with *Nco*I to target integration at *ura3*, yielding the *URA3:cla4-td* allele. To generate temperature-sensitive *cla4-75* strains, a 3.1 kb *Sac*I-*Hind*III fragment containing the *cla4-75* ORF together with 0.13 kb upstream and 0.38 kb downstream sequence [12] was cloned into the corresponding sites in YIplac128 [8], yielding pDLB2610. To generate analog-sensitive *cla4-*

as3 strains, a comparable 3.1 kb *Sal*I-*Hind*III *cla4-as3* fragment derived from the plasmid in strain DDY2056 [13] was cloned into YIplac128, yielding pDLB2602. A similar plasmid containing wild-type *CLA4* (pDLB2594) served as control. These plasmids were digested with *Bst*EII to target integration at *leu2*, yielding *LEU2:cla4-75*, *LEU2:cla4-as3*, and *LEU2:CLA4* alleles.

To generate a strain expressing Bem1p-GFP (DLY9070), we targeted homologous recombination of a plasmid containing a C-terminal fragment of *BEM1* fused to GFP (pDLB2968) at the wild-type *BEM1* locus. pDLB2968 contains *BEM1* sequences from nucleotide 754 within the ORF to 0.63 kb downstream of the ORF, cloned between *Xba*I (upstream) and *Xho*I (downstream) sites in pRS305 [5]. GFP coding sequences were inserted at the *BEM1* C-terminus using a previously described Bem1p-GFP fusion [14], which links the last residue of Bem1p to the second residue of GFP via the linker agactc, introducing a *Bgl*II site and encoding Arg Ser. At the GFP C-terminus there is a linker gcggccgctaagaagagttaacctcag containing a *Not*I site between the stop codon and *BEM1* downstream sequences. Integration was targeted to *BEM1* coding sequences by cutting at the unique *Pst*I site, which results in the replacement of the endogenous *BEM1* with *BEM1-GFP*, followed by an adjacent *LEU2* and promoterless C-terminal fragment of *BEM1* (designated as *BEM1-GFP:LEU2*). Correct integration in one chromosome of a wild-type diploid was verified by PCR tests, and sporulation and dissection was used to derive the final strains.

We also used CEN plasmids to express Bem1p-GFP. pDLB3162 contains *BEM1* sequences from 0.48 kb upstream of the start codon to the C-terminus, fused to GFP and 0.63 kb *BEM1* 3' untranslated sequence as described above, cloned between *Xba*I and *Xho*I sites in a pRS315 [5] backbone. pDLB2980 is a similar plasmid differing only in the junction between GFP and 3' sequences (*Pst*I instead of *Not*I).

To generate a strain expressing Bem1p^{P208L}-GFP (DLY9768), we targeted homologous recombination of a plasmid containing full-length *bem1*^{P208L}*-GFP* (pDLB2999) at the *BEM1* promoter of a chromosome in which the endogenous *BEM1* ORF had been deleted. pDLB2999 contains *bem1*^{P208L} sequences from 0.48 kb upstream of the ORF to 0.63 kb downstream of the ORF, cloned between *Xba*I (upstream) and *Xho*I (downstream) sites in pRS304 [5]. GFP coding sequences were inserted as described for pDLB2968 above, except for a different linker gcggccgccagtgtgatggatatctgcagaattcgcccttacgcgtcgac containing *Not*I, *Eco*RV, *Pst*I, *Eco*RI, and *Sal*I sites between the GFP stop codon and *BEM1* downstream sequences. Integration was targeted to the *BEM1* promoter of a *bem1::URA3* allele in a heterozygous diploid (DLY5029) by cutting at the unique *Sma*I site 210 bp upstream of the *BEM1* ORF. The resulting allele is designated *bem1*^{P208L}*-GFP:TRP1:bem1::URA3*. Correct integration was verified by PCR tests and tetrad analysis.

To generate strains expressing Bem1p-GFP-Cla4p, we targeted homologous recombination of a plasmid containing *BEM1* fused to GFP and then to an N-terminal fragment of *CLA4* (pDLB3038) at the wild-type *CLA4* locus. pDLB3038 contains *BEM1* sequences from 0.48 kb upstream of the start codon to the end of the ORF, fused to GFP via the linker agactc (introducing a *Bgl*II site and encoding Arg Ser between the last residue of Bem1p and the second residue of GFP), which in turn is fused to the first 785 nucleotides of the *CLA4* ORF via the linker gcggccgca (introducing a *Not*I site and encoding three alanines between the last residue of GFP and the start codon of Cla4p). The Bem1p-GFP-Cla4p sequences are cloned between *Xba*I (upstream) and *Xho*I (downstream) sites in pRS305. Digestion at the unique *Spe*I site in *CLA4* targets integration at the genomic *CLA4* locus, generating a full-length Bem1p-GFP-Cla4p fusion

expressed from the *BEM1* promoter and followed by *CLA4* downstream sequences. Adjacent to the fusion there are *LEU2* sequences and an N-terminal 785 nucleotide fragment of *CLA4* lacking the kinase domain. The resulting allele is designated *BEM1-GFP-CLA4:LEU2*. Analogous plasmids bearing point mutations in *BEM1* (pDLB3039, P208L; pDLB3040, K482A) were integrated in the same manner to express mutant fusion proteins. In the case of pDLB3039 this required partial digestion with *Spe*I as the P208L mutation introduces a second *Spe*I site [15].

To generate strains in which the Bem1p-GFP-Cla4p fusion is the only form of Bem1p present, integrations were performed in the heterozygous *bem1*::*URA3/BEM1* diploid DLY5029, successful integration was confirmed by PCR, and transformants were sporulated and dissected to obtain desired genotypes.

For unknown reasons, we were unable to detect the Bem1p-GFP-Cla4p fusion proteins by immunoblotting with an anti-GFP antibody, though we could detect them by fluorescence microscopy. To accurately assess their level of expression, the *Spe*I-digested plasmids pDLB3077, pDLB3078, and pDLB3079 (equivalent to pDLB3038, pDLB3039, and pDLB3040, except that they have a *TRP1* marker), were transformed into a strain expressing C-terminally myc-tagged Cla4p (DLY4003). In this case, integration yielded *BEM1-GFP-CLA4-myc* fusion proteins that were readily detected by immunoblotting with an anti-myc antibody, though they were still undetectable with anti-GFP. Given the lack of GFP immunoreactivity and the dimmer fluorescence from the GFP in this construct, we suspected that a mutation might have arisen in the GFP moiety during strain construction. However, sequencing of PCR products generated using the *BEM1-GFP-CLA4:LEU2* strain genomic DNA as template revealed a sequence identical to that in the *BEM1-GFP* plasmid originally obtained from M. Peter [14] and present in our other constructs. Thus, it appears that sandwiching GFP in between Bem1p and Cla4p renders it dimmer and less recognizable by the anti-GFP antisera.

To express Cdc24p-Bem1p-myc fusions, we generated plasmids containing *CDC24* sequences from 0.58 kb upstream of the start codon to nucleotide 2340 in the ORF (lacking the C-terminal PB1 domain), fused to Bem1p sequences downstream of nucleotide 418 in the ORF (lacking the N-terminal SH3 domain), followed by 12 myc tags and downstream terminator *SWE1* sequences derived from pDLB2226 [15]. This fusion (linking Cdc24p Ile780 to Bem1p Gly140) was cloned between blunted *Apa*I (upstream) and *Xho*I (downstream) sites in pRS315 [5], generating pDLB2561. Analogous plasmids were generated with mutations in the Bem1p SH3-2 (P208L, pDLB2562) and PB1 (K482A, pDLB2564) domains. All plasmids express the fusion proteins from the *CDC24* promoter. A control plasmid expressing Cdc24p$^{\Delta PB1}$ truncated at the same site as the fusions (pDLB2558) introduces the linker ggatcctga containing a *Bam*HI site and encoding Gly-Ser-Stop after Ile780.

To monitor localization of the Cdc24p-Bem1p fusion, we targeted integration of *CDC24-BEM1* at a genomic locus containing *BEM1-GFP*, yielding an integrated *CDC24-BEM1-GFP*. First, a *Sca*I-*Pst*I fragment from pDLB2561 (extending from 0.58 kb upstream of the start codon to nucleotide 975 in the *BEM1* ORF) was cloned into the corresponding sites in pRS304 [5], yielding pDLB3134. Digestion at the unique *Hpa*I site within *BEM1* was used to target integration of this plasmid at the *BEM1-GFP:LEU2* locus of DLY9070, yielding *TRP1:CDC24-BEM1-GFP:LEU2*.

To generate the Cdc24p-SH3-CI construct, we first cloned a *Bgl*II-*Not*I fragment containing GFP into *Bam*HI/*Not*I-cut pDLB2558, yielding pDLB3160 (expressing Cdc24p$^{\Delta PB1}$-GFP). A PCR product encoding the Bem1p SH3-2 domain (residues 140-257), followed by a

stop codon and 3' untranslated sequence from *CLA4* (480 bp immediately downstream of the stop codon) were then cloned between the *Not*I and *Sac*I sites of pDLB3160. The resulting plasmid, pDLB3161, expresses a protein consisting of Cdc24p residues 1-781 fused to GFP fused to Bem1p residues 140-257 from the *CDC24* promoter followed by *CLA4* 3' untranslated sequences. The Bem1p sequences in this construct extend a little beyond the minimal SH3-2 domain (residues 140-233), as we found that a similar construct containing only those sequences did not give rise to a stably expressed protein. Plasmids expressing Cdc24p-SH3^{P208L}-CI (pDLB3173) and Cdc24p-SH3-CI^{N253D} (pDLB3174) are identical to pDLB3161except for the indicated mutations which were introduced by site-directed mutagenesis. Residue numbers correspond to position in Bem1p and are not renumbered for the fusions.

To generate the Cdc24p-Cla4p fusion, we used the same approach described above to generate a plasmid similar to pDLB3161 except that it has a PCR product encoding the N-terminal 295 residues of Cla4p, instead of the Bem1p SH3-CI domain, between GFP and the *CLA4* 3'-UTR. This plasmid has a unique *Sal*I site at the junction between Cla4p coding sequences and the 3'-UTR, and we used gap repair in yeast to insert the remaining Cla4p sequences at that site. The resulting plasmid, pDLB3170, has a pRS315 backbone and expresses a protein consisting of Cdc24p residues 1-781 fused to GFP fused to full-length Cla4p followed by *CLA4* 3' untranslated sequences. Expression is driven by the *CDC24* promoter.

Because the Cdc24p-SH3-CI and Cdc24p-Cla4p fusions were made with a version of Cdc24p lacking the C-terminal Bem1p-binding PB1 domain of Cdc24p, we also generated a control Cdc24p$^{\Delta PB1}$-GFP construct by cloning a *Bgl*II-*Xho*I fragment containing GFP and *BEM1* 3' untranslated sequence of pDLB3162 into *Bam*HI/*Sal*I-cut pDLB2558, yielding pDLB3172.

Supplemental References

1. Chenevert, J., Corrado, K., Bender, A., Pringle, J., and Herskowitz, I. (1992). A yeast gene (*BEM1*) necessary for cell polarization whose product contains two SH3 domains. Nature *356*, 77-79.
2. Schenkman, L.R., Caruso, C., Page, N., and Pringle, J.R. (2002). The role of cell cycle-regulated expression in the localization of spatial landmark proteins in yeast. J Cell Biol *156*, 829-841.
3. Harkins, H.A., Page, N., Schenkman, L.R., De Virgilio, C., Shaw, S., Bussey, H., and Pringle, J.R. (2001). Bud8p and Bud9p, proteins that may mark the sites for bipolar budding in yeast. Mol Biol Cell *12*, 2497-2518.
4. Baudin, A., Ozier-Kalogeropoulos, O., Denouel, A., Lacroute, F., and Cullin, C. (1993). A simple and efficient method for direct gene deletion in *Saccharomyces cerevisiae*. Nucleic Acids Res. *21*, 3329-3330.
5. Sikorski, R.S., and Hieter, P. (1989). A system of shuttle vectors and yeast host strains designed for efficient manipulation of DNA in *Saccharomyces cerevisiae*. Genetics *122*, 19-27.
6. Goldstein, A.L., and McCusker, J.H. (1999). Three new dominant drug resistance cassettes for gene disruption in *Saccharomyces cerevisiae*. Yeast *15*, 1541-1553.
7. Bender, L., Shuen Lo, H., Lee, H., Kokojan, V., Peterson, J., and Bender, A. (1996). Associations among PH and SH3 domain-containing proteins and Rho-type GTPases in yeast. J. Cell Biol. *133*, 879-894.

8. Gietz, R.D., and Sugino, A. (1988). New yeast-*Escherichia coli* shuttle vectors constructed with in vitro mutagenized yeast genes lacking six base pair restriction sites. Gene *74*, 527-534.
9. Winters, M.J., and Pryciak, P.M. (2005). Interaction with the SH3 domain protein Bem1 regulates signaling by the Saccharomyces cerevisiae p21-activated kinase Ste20. Mol Cell Biol *25*, 2177-2190.
10. Leberer, E., Wu, C., Leeuw, T., Fourest-Lieuvin, A., Segall, J.E., and Thomas, D.Y. (1997). Functional characterization of the Cdc42p binding domain of yeast Ste20p protein kinase. EMBO J. *16*, 83-97.
11. Holly, S.P., and Blumer, K.J. (1999). PAK-Family Kinases Regulate Cell and Actin Polarization throughout the Cell Cycle of Saccharomyces cerevisiae. J Cell Biol *147*, 845-856.
12. Cvrckova, F., De Virgilio, C., Manser, E., Pringle, J.R., and Nasmyth, K. (1995). Ste20-like protein kinases are required for normal localization of cell growth and for cytokinesis in budding yeast. Genes Dev. *9*, 1817-1830.
13. Weiss, E.L., Bishop, A.C., Shokat, K.M., and Drubin, D.G. (2000). Chemical genetic analysis of the budding-yeast p21-activated kinase Cla4p. Nat. Cell Biol *2*, 677-685.
14. Butty, A.C., Perrinjaquet, N., Petit, A., Jaquenoud, M., Segall, J.E., Hofmann, K., Zwahlen, C., and Peter, M. (2002). A positive feedback loop stabilizes the guanine-nucleotide exchange factor Cdc24 at sites of polarization. Embo J *21*, 1565-1576.
15. Irazoqui, J.E., Gladfelter, A.S., and Lew, D.J. (2003). Scaffold-mediated symmetry breaking by Cdc42p. Nat Cell Biol *5*, 1062-1070.
16. Bi, E., and Pringle, J.R. (1996). *ZDS1* and *ZDS2*, genes whose products may regulate Cdc42p in *Saccharomyces cerevisiae*. Mol. Cell. Biol. *16*, 5264-5275.
17. Bose, I., Irazoqui, J.E., Moskow, J.J., Bardes, E.S., Zyla, T.R., and Lew, D.J. (2001). Assembly of scaffold-mediated complexes containing Cdc42p, the exchange factor Cdc24p, and the effector Cla4p required for cell cycle-regulated phosphorylation of Cdc24p. J Biol Chem *276*, 7176-7186.
18. Saito, K., Fujimura-Kamada, K., Hanamatsu, H., Kato, U., Umeda, M., Kozminski, K.G., and Tanaka, K. (2007). Transbilayer phospholipid flipping regulates Cdc42p signaling during polarized cell growth via Rga GTPase-activating proteins. Dev Cell *13*, 743-751.
19. Nern, A., and Arkowitz, R.A. (1999). A Cdc24p-Far1p-Gbetagamma protein complex required for yeast orientation during mating. J Cell Biol *144*, 1187-1202.

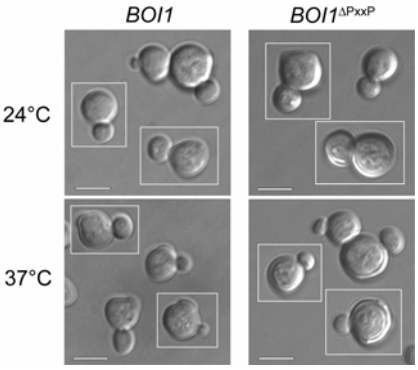

Figure S1. Boi1p-Bem1p interaction is not required for symmetry-breaking polarization. Cells recovered from the 5-FOA plates described in Fig. 1B were grown at 24°C or at 37°C for 5 h in medium lacking leucine. At both temperatures, the cell morphology of cells carrying *BOI1*$^{\Delta PxxP}$ was indistinguishable from that of cells carrying wild-type *BOI1*. Boxes denote cells from different fields. Bars, 5 μm.

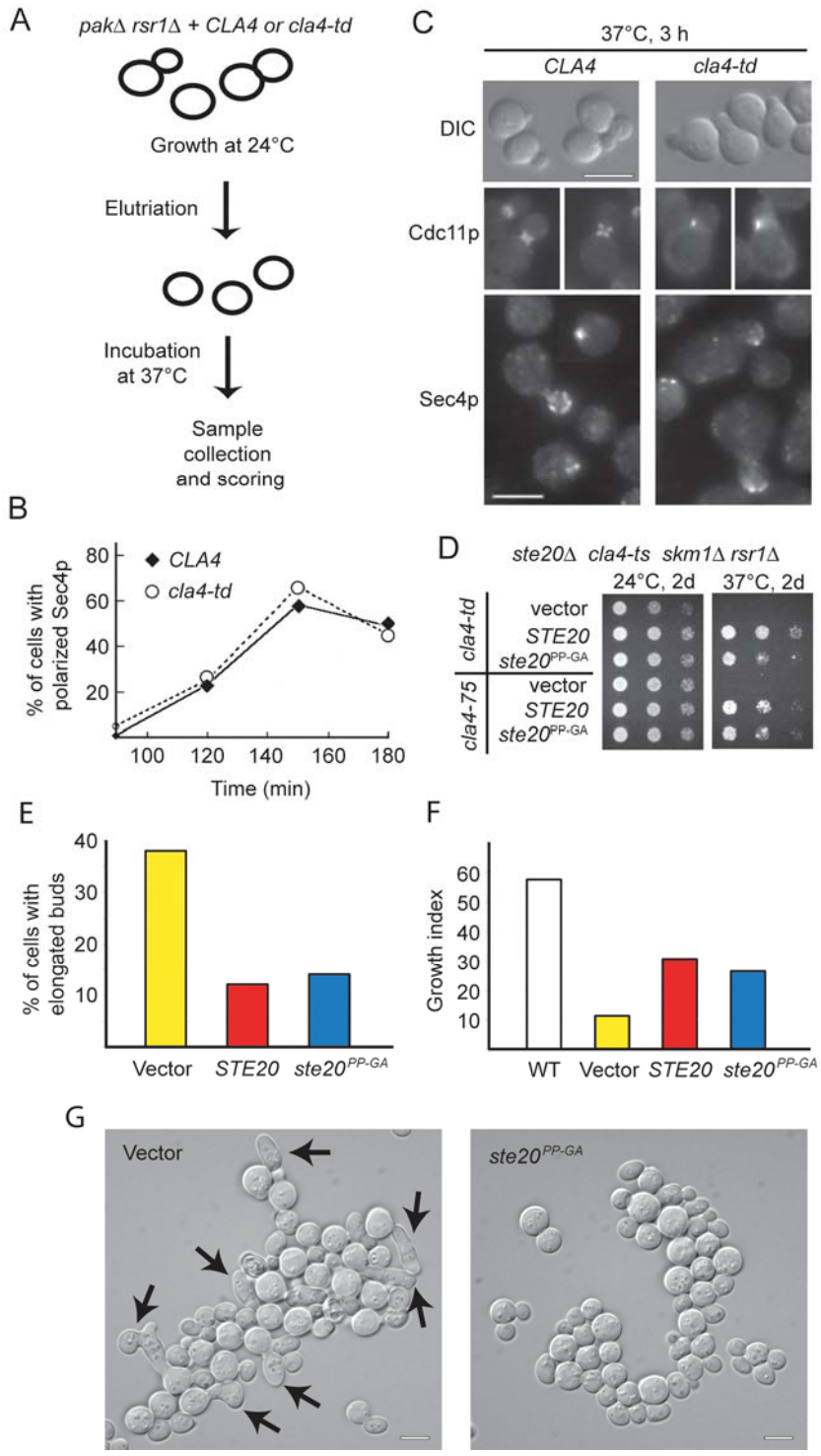

Figure S2. Conditional *cla4* mutants retain residual function and break symmetry under restrictive conditions.

(A) Schematic of the experimental procedure. *rsr1*Δ *skm1*Δ *ste20*Δ *cla4*Δ *cla4-td* cells (DLY7853) were grown in YEPSucrose medium at 24°C to 2x10^7 cells/ml, and unbudded daughter cells were isolated from the population by centrifugal elutriation. Following Holly and

Blumer [11], the cells were then incubated at 37°C in media lacking sugar for 1 h to allow for slow degradation of the degron-Cla4p. Cells were then resuspended in YEPD at 37°C and samples were collected every 30 min. (Similar results were obtained if the sugarless pre-incubation step was omitted, and with the *cla4-75* allele as well as the *cla4-td* allele). **(B)** Because cells lacking PAKs do not make normal buds [12], we scored polarization by monitoring the distribution of the secretory vesicle marker Sec4p. Sec4p localization was examined by indirect immunofluorescence and the number of cells with polarized Sec4p was scored (n>200 for each sample). **(C)** Representative examples of cell morphology (DIC, top), septin distribution (Cdc11p, middle), and Sec4p distribution (bottom) after 3 h in YEPD at 37°C. *cla4-td* displayed polarized Sec4p but disorganized septins and aberrant cell shape. Bars, 5 μm. **(D)** Ste20p$^{PP\text{-}GA}$ can promote growth of *rsr1*Δ strains containing temperature-sensitive Cla4p at restrictive temperature. Strains containing either of two published PAK temperature-sensitive alleles (*cla4-75* [12] or *cla4-td* [11]) as the only PAK (*cla4-td*, DLY7853; *cla4-75*, DLY7782) were transformed with plasmids containing either *STE20* (pDLB2922, pPP2370), *ste20*$^{PP\text{-}GA}$ (pDLB2923, pDLB2921), or the vector control. Transformants were grown overnight at 24°C, spotted onto plates, and incubated for 2 d at 24°C (left) or 37°C (right). **(E)** Ste20p$^{PP\text{-}GA}$ can suppress the elongated-bud phenotype of *rsr1*Δ strains containing analog-sensitive Cla4p in the presence of inhibitor. A strain containing *cla4-as3* [13] as the only PAK (DLY7728) was transformed with plasmids containing either *STE20* (pPP2370), *ste20*$^{PP\text{-}GA}$ (pDLB2921), or the vector control. Transformants were grown initially in selective medium, inoculated at ~10^7 cells/ml into YEPD supplemented with 25 μM 1NM-PP1 or DMSO as control, and grown for 6 h at 30°C. The percentage of cells with elongated bud morphology was scored (n>150). In this strain background the elongated-bud phenotype is not fully penetrant, but suppression by Ste20$^{PP\text{-}GA}$ is nevertheless apparent and comparable to that of wild-type Ste20p. **(F)** Ste20p$^{PP\text{-}GA}$ can suppress the growth defect of *rsr1*Δ strains containing analog-sensitive Cla4p in the presence of inhibitor. The strains from (E) and an additional control wild type strain (DLY1273, grown for 6.5 h) were treated as described above and growth inhibition by 1NM-PP1 is represented by a growth index, which represents the % cell number increase in 25 μM 1NM-PP1 as compared to DMSO. In this genetic background, even the wild-type strain was partially growth-inhibited by 1-NM-PP1, though to a much lesser extent than the analog-sensitive control (vector). Ste20$^{PP\text{-}GA}$ was able to suppress the growth defect to an extent comparable to that of wild-type Ste20p. **(G)** DIC images of representative cells treated as above, illustrating aberrant morphologies including elongated buds (arrows) that are suppressed in the presence of Ste20p$^{PP\text{-}GA}$. DLY7728 transformed with vector (left) or pDLB2921 (right). Bars, 5 μm.

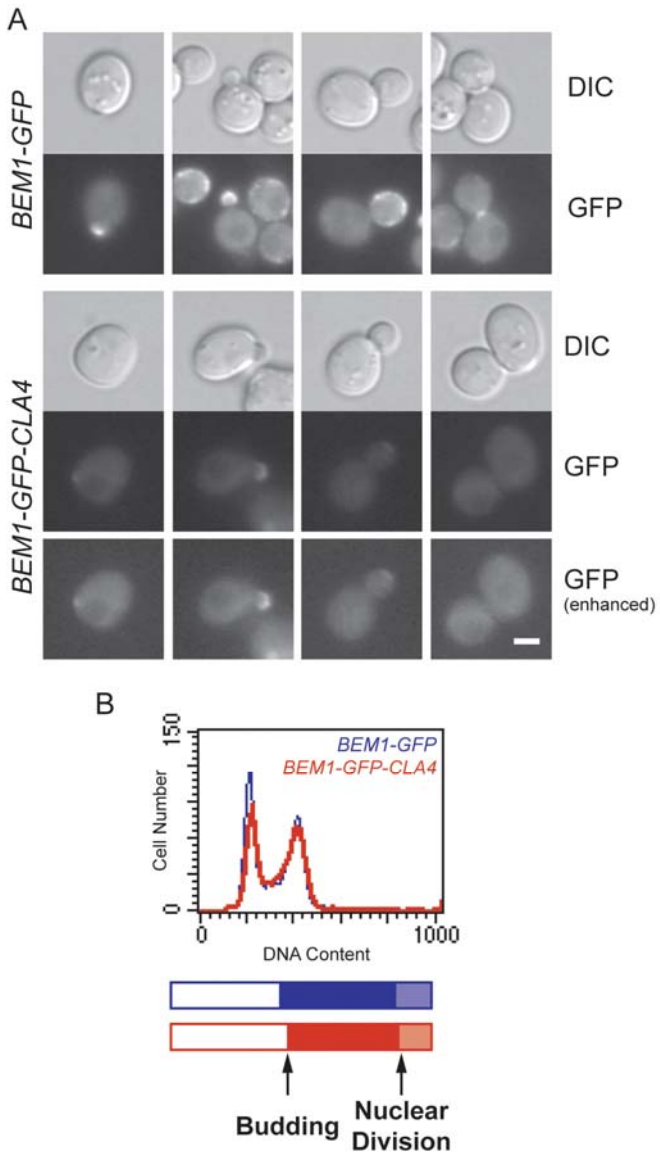

Figure S3. Subcellular localization and function of Bem1p-Cla4p fusion protein.
(A) Bem1p-Cla4p is concentrated at the presumptive bud site. Strains expressing *BEM1-GFP* (DLY9046) or *BEM1-GFP-CLA4* (DLY9962) were grown in synthetic medium at 24°C. DIC and GFP images of representative living cells from different stages of the cell cycle are shown, taken on the same day with identical processing. Because the Bem1p-GFP-Cla4p construct was dimmer, the same pictures are shown after Photoshop enhancement in the bottom row. Unlike Bem1p, Bem1p-Cla4p does not concentrate at the neck during cytokinesis. Bar, 1 μm. **(B)** Bem1p-Cla4p promotes robust growth and cell cycle progression. FACS profiles are shown for *BEM1-GFP rsr1Δ* (blue, DLY9165, doubling time 104 min) and *BEM1-GFP-CLA4 rsr1Δ* (red, DLY9967, doubling time 110 min) cells grown in YEPD at 30°C. The proportion of unbudded cells, budded cells with a single nucleus, and budded cells after nuclear division in an asynchronous culture was determined by scoring DAPI-stained cells (n>500), and is shown as a cell cycle timeline representing when an "average cell" in the population buds and undergoes nuclear division.

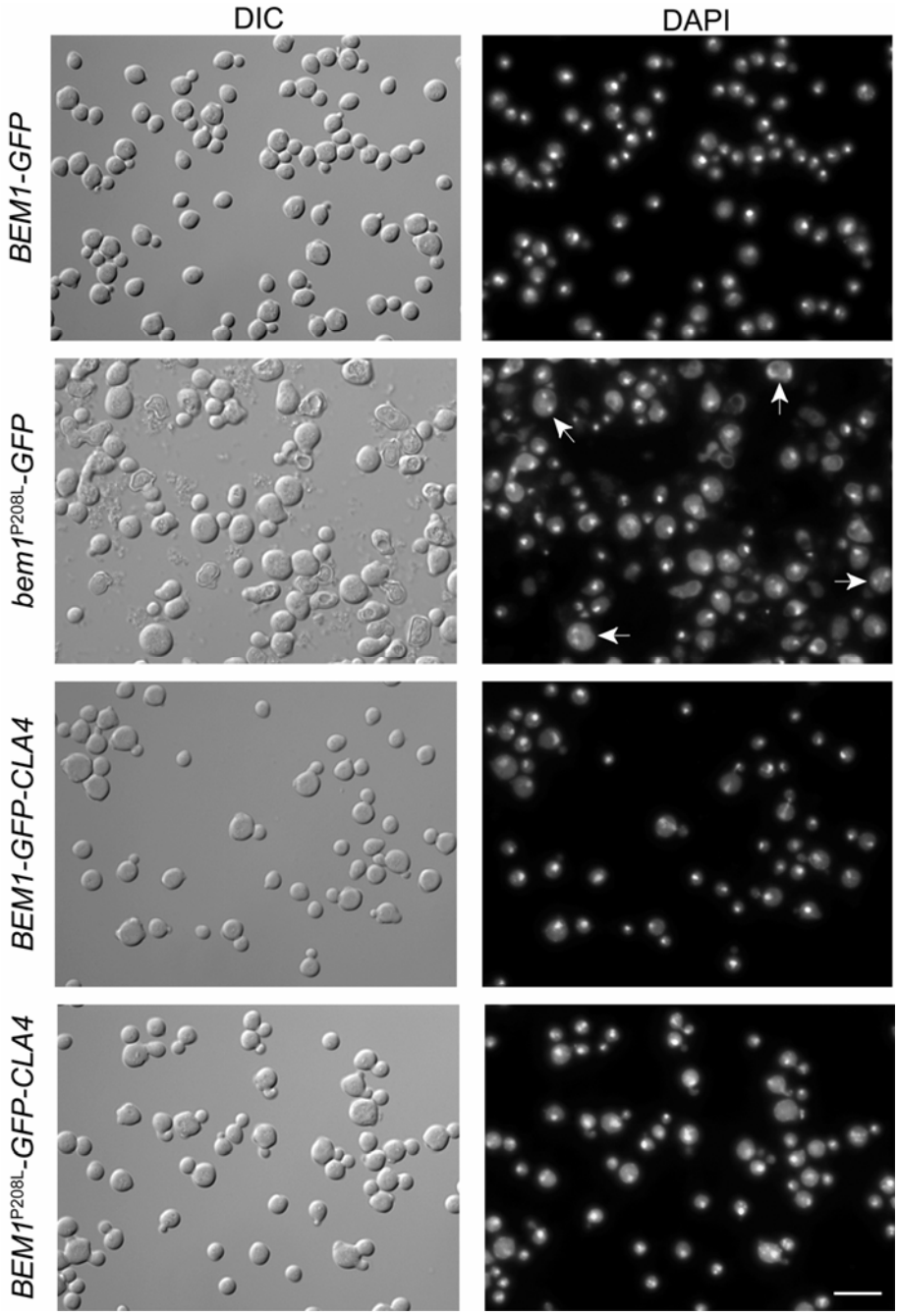

Figure S4. Morphology and multinucleate phenotypes of *bem1*^{P208L} are rescued by fusion to *CLA4*.

*rsr1*Δ strains expressing either *BEM1-GFP* (DLY8014), *bem1*^{P208L}*-GFP* (DLY9768), *BEM1-GFP-CLA4* (DLY9966) or *BEM1*^{P208L}*-GFP-CLA4* (DLY9978) as the sole source of Bem1p were grown in YEPD medium at 24°C, shifted to 37°C for 10 h, and fixed for analysis of cell morphology (DIC) and DNA staining (DAPI). Only *bem1*^{P208L}*-GFP* cells displayed a high frequency of large, lysed, and multinucleate (arrows) cell phenotypes indicative of polarity defects. Bar, 10 μm.

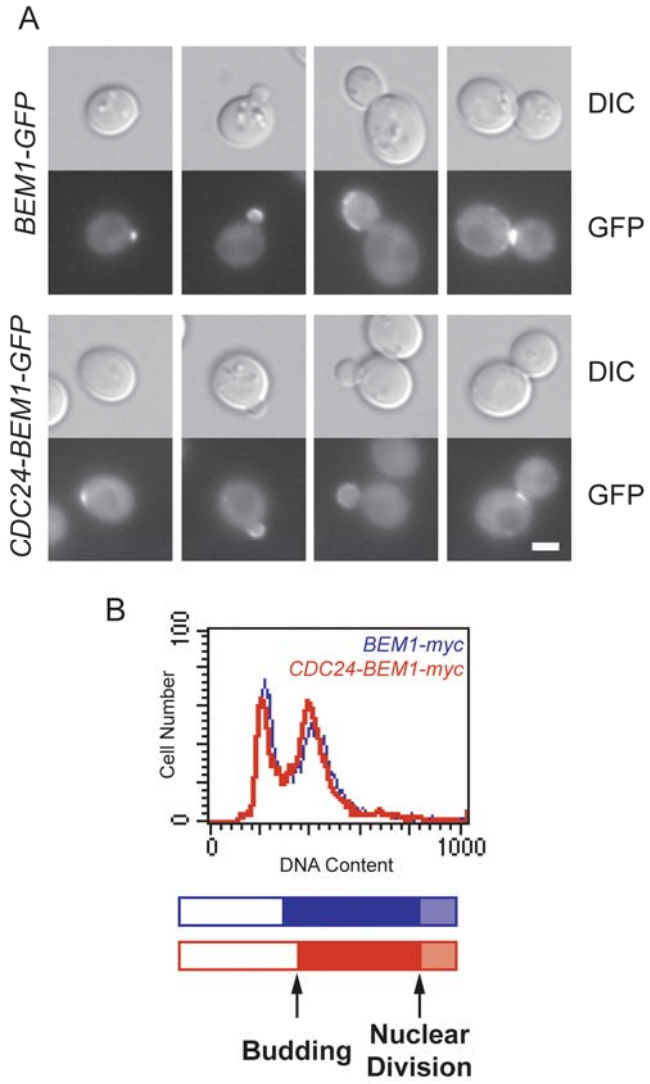

Figure S5. Subcellular localization and function of Cdc24p-Bem1p fusion protein.
(A) Cdc24p-Bem1p is concentrated at the presumptive bud site. Strains expressing *BEM1-GFP* (DLY9046) or *CDC24-BEM1-GFP* (DLY9912) were grown in synthetic medium at 24°C. DIC and GFP images of representative living cells from different stages of the cell cycle are shown, taken on the same day with identical processing. Bar, 1 μm. **(B)** Cdc24p-Bem1p promotes robust growth and cell cycle progression. FACS profiles for *BEM1-myc rsr1Δ* (blue, DLY10021, doubling time 141 min) and *CDC24-BEM1-myc rsr1Δ* (red, DLY10036, doubling time 128 min) grown at 30°C in synthetic medium lacking leucine to select for plasmid maintenance. The proportion of unbudded cells, budded cells with a single nucleus, and budded cells after nuclear division in an asynchronous culture was determined by scoring DAPI-stained cells (n>500), and is shown as a cell cycle timeline representing when an "average cell" in the population buds and undergoes nuclear division.

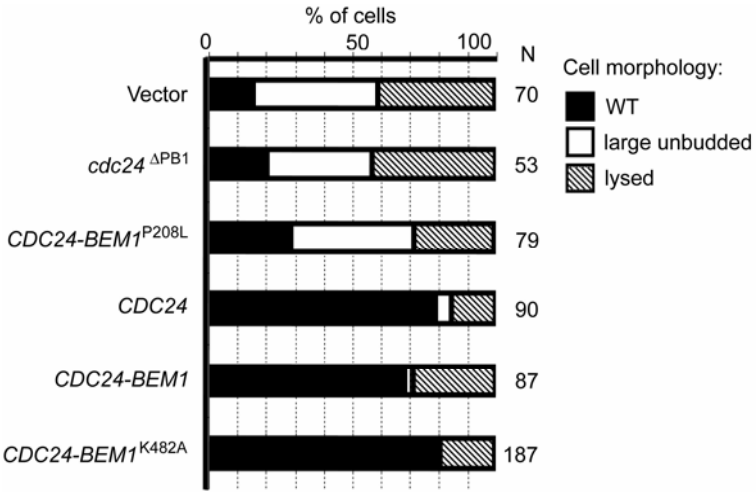

Figure S6. Rescue of *cdc24-1* polarity defects by Cdc24p-Bem1p fusion proteins. A *cdc24-1* strain (DLY4032) was transformed with plasmids expressing either Cdc24p (DLB2557), Cdc24p$^{\Delta PB1}$ (DLB2558), Cdc24p-Bem1p (DLB2561), Cdc24p-Bem1p^{K482A} (DLB2564), Cdc24p-Bem1p^{P208L} (DLB2562), or vector control. Cells were grown in selective medium and shifted to 37ºC for 5 h. At this temperature, *cdc24-1* mutants accumulate as large round unbudded cells that eventually lyse. Cells in DIC images (cell number N indicated) were scored as WT (black: normal size, either budded or unbudded), large round unbudded (white), or lysed (hatched). Whereas Cdc24p-Bem1p and Cdc24p-Bem1p^{K482A} provided a rescue comparable to the Cdc24p control, Cdc24p$^{\Delta PB1}$ and Cdc24p-Bem1p^{P208L} failed to rescue and appeared comparable to the vector control.

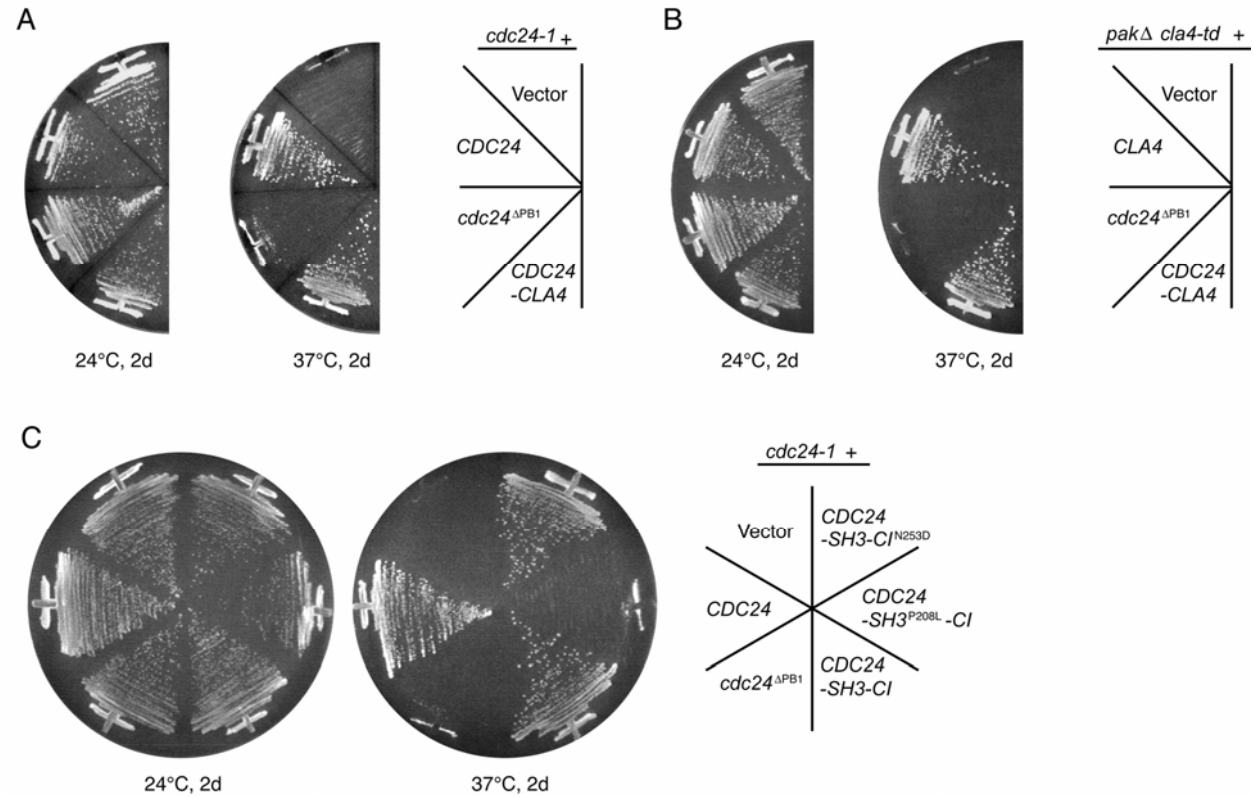

Figure S7. Functional characterization of Cdc24p-Cla4p and Cdc24p-SH3-CI proteins. **(A)** Cdc24p-Cla4p complements the lethality of a *cdc24-1* strain at 37°C. Strain DLY4032 was transformed with pRS315 (vector), pDLB2557 (*CDC24*), pDLB2558 (*cdc24*$^{\Delta PB1}$), or pDLB3170 (*CDC24-CLA4*) and streaked on selective media at 24°C (left) or 37°C (right). Plates were incubated for 2 d. **(B)** Cdc24p-Cla4p complements the lethality of a *cla4*Δ *ste20*Δ *skm1*Δ *cla4-td* strain at 37°C. Strain DLY7877 was transformed with pRS315 (vector), pDLB2638 (*CLA4*), pDLB2558 (*cdc24*$^{\Delta PB1}$), or pDLB3170 (*CDC24-CLA4*) and analyzed as in (A). **(C)** Cdc24p-SH3-CI, but not a version that lacks a functional SH3 domain, complements the lethality of a *cdc24-1* strain at 37°C. Strain DLY4032 was transformed with pRS315 (vector), pDLB2557 (*CDC24*), pDLB2558 (*cdc24*$^{\Delta PB1}$), pDLB3161 (*CDC24-SH3-CI*), pDLB3173 (*CDC24-SH3*^{P208L}*-CI*), or pDLB3174 (*CDC24-SH3-CI*^{N253D}) and analyzed as in A). None of the constructs contain the endogenous Cdc24p PB1 domain (see Fig. 4A and 5A schematics). The SH3 mutation is at the residue corresponding to P208 in Bem1p, and the CI mutation is at the residue corresponding to N253 in Bem1p.

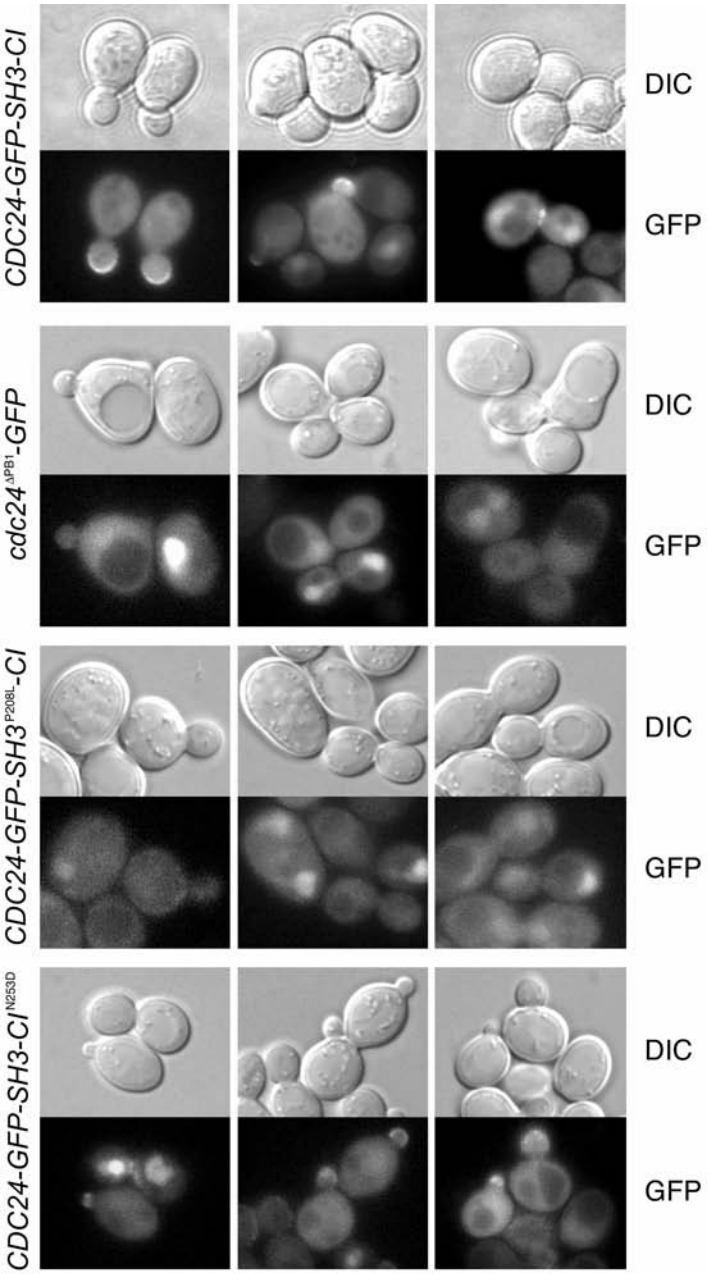

Figure S8. Subcellular localization of Cdc24p-SH3-CI proteins.

DIC and GFP images of *cdc24-1* cells (DLY4032) expressing Cdc24p-GFP-SH3-CI (top, pDLB3161), or related constructs lacking the SH3-CI (second row, pDLB3172), or mutated in the SH3 domain (third row, pDLB3173) or in the CI domain (bottom row, pDLB3174). Cells were grown in synthetic medium and shifted to 37°C for 5 h to inactivate the endogenous Cdc24-1p. Images of representative living cells from different stages of the cell cycle are shown, taken on the same day.

Table S1. Yeast strains

Strain	***Relevant genotype***	***Source***
DLY649[a]	α *cdc24-4*	This study
DLY1273	**a** (YEF473)	[16]
DLY4000[b]	**a** *BEM1-myc:HIS3*	[17]
DLY4003[b]	**a** *CLA4-myc:URA3*	This study
DLY4032[b]	**a** *cdc24-1 HIS2 his3*	This study
DLY5029	**a**/α *rsr1::HIS3/ rsr1::HIS3 bem1::URA3/BEM1*	This study
DLY7606	**a** *rsr1::HIS3 bud8::TRP1 cla4::nat^{R} ste20::URA3 skm1::kan^{R} LEU2:CLA4*	This study
DLY7728	**a** *rsr1::HIS3 bud8::TRP1 cla4::nat^{R} ste20::hyg^{R} skm1::kan^{R} LEU2:cla4-as3*	This study
DLY7782	α *rsr1::HIS3 bud8::TRP1 cla4::nat^{R} ste20::hyg^{R} skm1::kan^{R} LEU2:cla4-75*	This study
DLY7853	α *rsr1::HIS3 bud8::TRP1 cla4::nat^{R} ste20::hyg^{R} skm1::kan^{R} URA3:cla4-td*	This study
DLY7877	α *cla4::nat^{R} ste20::hyg^{R} skm1::kan^{R} URA3:cla4-td*	This study
DLY7891	α *rsr1::HIS3 bud8::TRP1 boi2::kan^{R} boi1::hyg^{R}* 2 μm *BOI2 URA3*	This study
DLY8014	**a** *BEM1-GFP:URA3 rsr1::HIS3*	This study
DLY8798	**a** *cla4::nat^{R} STE20^{PP-GA} skm1::kan^{R} bud8::TRP1*	This study
DLY9046[b]	α *BEM1-GFP:LEU2*	This study
DLY9070	α *BEM1-GFP:LEU2*	This study
DLY9165	α *BEM1-GFP:LEU2 rsr1::TRP1*	This study
DLY9474[b]	α *cla4::nat^{R} ste20::hyg^{R} skm1::TRP1 rsr1::kan^{R}* 2 μm *CLA4 URA3*	This study
DLY9478[b]	**a** *cla4::nat^{R} ste20::hyg^{R} rsr1::kan^{R}* 2 μm *CLA4 URA3*	This study
DLY9479[b]	**a** *cla4::nat^{R} ste20::hyg^{R} skm1::TRP1* 2 μm *CLA4 URA3*	This study
DLY9768	α *bem1^{P208L}-GFP:TRP1:bem1::URA3 rsr1::HIS3*	This study
DLY9837[b]	**a** *BEM1^{P208L}-GFP-CLA4-myc:TRP1:URA3*	This study
DLY9838[b]	**a** *BEM1^{K482A}-GFP-CLA4-myc:TRP1:URA3*	This study
DLY9912[b]	α *CDC24-BEM1-GFP:TRP1:LEU2*	This study
DLY9962[b]	**a** *BEM1-GFP-CLA4-myc:TRP1:URA3*	This study
DLY9963	**a**/α *BEM1-GFP-CLA4:LEU2/CLA4 bem1::URA3/BEM1 rsr1::HIS3/rsr1::HIS3*	This study
DLY9966	**a** *BEM1-GFP-CLA4:LEU2 bem1::URA3 rsr1::HIS3*	This study
DLY9967	α *BEM1-GFP-CLA4:LEU2 bem1::URA3 rsr1::HIS3*	This study
DLY9968	**a**/α *BEM1^{K482A}-GFP-CLA4:LEU2/CLA4 bem1::URA3/BEM1 rsr1::HIS3/ rsr1::HIS3*	This study
DLY9975	**a**/α *BEM1^{P208L}-GFP-CLA4:LEU2/CLA4 bem1::URA3/BEM1 rsr1::HIS3/ rsr1::HIS3*	This study
DLY9978	**a** *BEM1 ^{P208L}-GFP-CLA4:LEU2 bem1::URA rsr1::HIS3*	This study
DLY10021	α *rsr1::HIS3 bem1::URA3* YEpLac181-*BEM1-myc*	This study
DLY10032	**a** *rsr1::HIS3 bem1::URA3* YEpLac181-*bem1^{K482A}-myc*	This study

DLY10034	*rsr1::HIS3 bem1::URA3* pRS315-*CDC24-BEM1*$_{K482A}$*-myc*	This study
DLY10036	*rsr1::HIS3 bem1::URA3 pRS315-CDC24-BEM1-myc*	This study
DLY11010	**a** *rsr1::HIS3 bem1::URA3 pRS315-BEM1-GFP*	This study
DLY11011	**a** *rsr1::HIS3 bem1::URA3 pRS315-CDC24-GFP-SH3-CI*	This study
DLY11101	**a** *rsr1::HIS3 bem1::URA3 pRS315-CDC24-GFP-CLA4*	This study

All strains are in the YEF473 background (*his3-*Δ*200 leu2-*Δ*1 lys2-801 trp1-*Δ*63 ura3-52*), except as marked below.

[a] The *cdc24-4* mutation was back-crossed 3 times into the BF264-15Du strain background.

[b] These strains are in the BF264-15Du (Richardson *et al*., 1989) background (*ade1 his2 leu23,112 trp1-1 ura3*Δ*ns*)

Table S2. Plasmids used in this study

Plasmid	Description	Source
	BOI1 & BOI2	
pDLB2647	*BOI1*$^{\Delta PxxP}$ *CEN LEU2*	This study
pDLB2648	*BOI1 CEN LEU2*	This study
pPB1071	*BOI2 2μm URA3*	A. Bender
	STE20 & CLA4	
pRL116	*GFP-STE20 CEN URA3*	[10]
pPP1211	*GFP-STE20*$^{PP-GA}$ *CEN URA3*	[9]
pPP2370	*STE20 CEN URA3*	P.Pryciak
pDLB2921	*STE20*$^{PP-GA}$ *CEN URA3*	This study
pDLB2922	*STE20 CEN LEU2*	This study
pDLB2923	*STE20*$^{PP-GA}$ *CEN LEU2*	This study
pDLB722	*CLA4 2μm URA3*	E. Bi
pDLB2638	*CLA4 CEN LEU2*	This study
pDLB2396	*CLA4 CEN TRP1*	E. Weiss
pDLB3080	*CLA4 2μm TRP1*	This study
pDLB2398	*cla4*^{D693A} *CEN TRP1*	E. Weiss
pDLB2594	*CLA4 LEU2*	This study
p*cla4-td*	*cla4-td URA3*	[11]
pDLB2610	*cla4-75 LEU2*	This study
pDLB2602	*cla4-as3 LEU2*	This study
	BEM1	
pDLB2374	*BEM1-myc 2μm LEU2*	[15]
pDLB2375	*bem1*^{P208L}*-myc 2μm LEU2*	[15]
pDLB2379	*bem1*^{K482A}*-myc 2μm LEU2*	[15]
pDLB2968	*BEM1(C-term)-GFP LEU2*	This study
pDLB2980	*BEM1-GFP CEN LEU2*	This study
pDLB3162	*BEM1-GFP CEN LEU2*	This study
pDLB3140	*BEM1-GFP CEN TRP1*	This study
pDLB2981	*bem1*^{P208L}*-GFP CEN LEU2*	This study
pDLB2999	*bem1*^{P208L}*-GFP TRP1*	This study
	CDC24-BEM1	
pDLB2561	*CDC24-BEM1-myc CEN LEU2*	This study
pDLB2562	*CDC24-BEM1*^{P208L}*-myc CEN LEU2*	This study
pDLB2564	*CDC24-BEM1*^{K482A}*-myc CEN LEU2*	This study
pDLB3134	*CDC24-BEM1(N-term)*	This study
	BEM1-CLA4	
pDLB3038	*BEM1-GFP-CLA4(N-term) LEU2*	This study
pDLB3039	*BEM1*^{P208L}*-GFP-CLA4(N-term) LEU2*	This study
pDLB3040	*BEM1*^{K482A}*-GFP-CLA4(N-term) LEU2*	This study

pDLB3077	*BEM1-GFP-CLA4(N-term) TRP1*	This study
pDLB3078	*BEM1*^{P208L}*-GFP-CLA4(N-term) TRP1*	This study
pDLB3079	*BEM1*^{K482A}*-GFP-CLA4(N-term) TRP1*	This study
	CDC24	
pDLB2557	*CDC24 CEN LEU2*	This study
pDLB2558	*cdc24*$^{\Delta PB1}$ *CEN LEU2*	This study
pDLB3172	*cdc24*$^{\Delta PB1}$*-GFP CEN LEU2*	This study
pDLB3159	*GFP-CDC24 CEN LEU2*	[18]
pDLB1303	*CDC24-HA-GFP CEN TRP1*	[19]
pDLB3161	*CDC24-GFP-SH3-CI CEN LEU2*	This study
pDLB3173	*CDC24-GFP-SH3* ^{P208L}*-CI CEN LEU2*	This study
pDLB3174	*CDC24-GFP-SH3-CI* ^{N253D} *CEN LEU2*	This study
pDLB3170	*CDC24-GFP-CLA4 CEN LEU2*	This study